$Pb_5Bi_{24}Se_{41}$: A New Member of the Homologous Series Forming Topological Insulator Heterostructures

Kouji Segawa, A. A. Taskin, Yoichi Ando*

Institute of Scientific and Industrial Research, Osaka University
8-1 Mihogaoka, Ibaraki, Osaka 567-0047, Japan

arXiv:1411.5462v1 [cond-mat.mtrl-sci] 20 Nov 2014

Abstract

We have synthesized $Pb_5Bi_{24}Se_{41}$, which is a new member of the $(PbSe)_5(Bi_2Se_3)_{3m}$ homologous series with $m = 4$. This series of compounds consist of alternating layers of the topological insulator Bi_2Se_3 and the ordinary insulator PbSe. Such a naturally-formed heterostructure has recently been elucidated to give rise to peculiar quasi-two-dimensional topological states throughout the bulk, and the discovery of $Pb_5Bi_{24}Se_{41}$ expands the tunability of the topological states in this interesting homologous series. The trend in the resistivity anisotropy in this homologous series suggests an important role of hybridization of the topological states in the out-of-plane transport.

Keywords: topological insulator, bismuth selenide, crystal growth, quasi-two-dimensional transport

1. Introduction

Topological insulators (TIs) are a new class of materials characterized by a nontrivial topology of the Hilbert space spanned by the wave functions of the occupied electronic states [1, 2, 3]. They are expected to be useful for various applications including high-frequency electronics, transparent electrodes, spintronics, and quantum computations [4, 5, 6]. Already a number of bulk materials have been found to be three-dimensional (3D) TIs [3], and they are all narrow-gap semiconductors composed of heavy elements which cause band inversions [3, 6]. When the band inversion occurs at an odd number of the high-symmetry points in the Brillouin zone, the topological principle [3] dictates that charge-conducting gapless states show up on the surface. Hence, 3D TIs are peculiar in that they consist of gapped bulk states accompanied by gapless surface states of topological origin. Syntheses of new 3D TI materials are of great current interest for expanding our knowledge about the relationship between chemistry and quantum-mechanical functionalities [6].

In this context, there is an intriguing class of materials whose crystal structures realize a naturally-formed heterostructure consisting of alternating layers of topological insulators and ordinary insulators [3]; due to their constructions, such materials can be considered to lie at the boundary between topologically trivial and nontrivial materials. Specifically, in the homologous series of Pb-Bi-Se ternary compounds expressed in the formula $(PbSe)_5(Bi_2Se_3)_{3m}$ [7, 8, 9], which we call PSBS here, layers of PbSe (which is an ordinary insulator) alternate with layers of Bi_2Se_3 (which is a prototypical topological insulator [10]). In these series of compounds, it was inferred from the band structure data obtained from angle-resolved photoemission spectroscopy (ARPES) that each internal interface between PbSe and Bi_2Se_3 layers harbor topological interface states, leading to the situation that the whole bulk is filled with quasi-two-dimensional states of topological origin [11].

Interestingly, since the topological interface states appear on both sides of each Bi_2Se_3 layer sandwiched by PbSe layers, the two topological states at the top and bottom interfaces can hybridize *within* each Bi_2Se_3 layer, leading to the opening of a gap in the topological states [11]. The size of this hybridization gap becomes smaller as the Bi_2Se_3 layer becomes thicker and the hybridization becomes weaker. Based on the electronic structure data obtained from ultrathin films of Bi_2Se_3 [12], it is expected that the hybridization is gone when the Bi_2Se_3 layer becomes thicker than 5 nm. Note that the crystal structure of Bi_2Se_3 consists of covalently-bonded Se-Bi-Se-Bi-Se quintuple layers (QLs) that are interconnected by weak van der Waals force [3]. The thickness of each QL is 0.9545 nm. Thus, the hybridization of topological states in PSBS would disappear when each Bi_2Se_3 layer contains more than 5 QLs.

In the $(PbSe)_5(Bi_2Se_3)_{3m}$ homologous series, the parameter m gives the number of QLs included in each Bi_2Se_3 layer, and the topological states becomes more robust for larger m. So far, syntheses of compounds with $m = 1$, 2, and 3 have been reported [7, 8, 9, 13], and it is naively expected that, based on the phase diagram of the PbSe-Bi_2Se_3 pseudo-binary system reported by Shelimova *et al.* [9], compounds with larger m would not be naturally synthesized because they are not thermodynamically stable. Despite this naive expectation, we have successfully synthesized $m = 4$ compound based on a melt-growth strategy in which the composition of the melt changes continuously as the growth proceeds. The expansion of the available compounds in this interesting homologous series is useful, because one can tune the hybridization of the topological states by changing m, which is a unique tunability among topological materials. In this paper, we report the synthesis and analyses of the $Pb_5Bi_{24}Se_{41}$ [$= (PbSe)_5(Bi_2Se_3)_{12}$, called PSBS $m = 4$] compound, as well as its anisotropic transport properties which support the quasi-two-dimensional nature of its electronic states.

2. Materials and methods

2.1. Experimental Methods

The X-ray diffraction (XRD) analysis using 2θ–θ scan is performed with Rigaku Ultima-IV X-ray apparatus equipped with a 1D-detector. For single-crystal X-ray analysis, Rigaku Mercury CCD system with graphite-monochromated MoKα radiation is used. The in-plane transport properties of PSBS single crystals are measured by standard ac six-probe method, which allows measurements of the in-plane resistivity ρ_{ab} and the Hall resistivity $\rho_{\rm H}$ at the same time. By sweeping the magnetic field up to ± 2 T, the linear slope of $\rho_{\rm H}$ vs. B is obtained, from which the Hall coefficient $R_{\rm H}$ is calculated. The out-of-plane resistivity ρ_{c^*} is measured by using a four-probe method, in which the current and voltage contacts are made near the edges of the top and bottom surfaces of a rectangular sample. In the present work, ρ_{ab} and ρ_{c^*} are measured on the same samples to avoid unnecessary complications, and the results from several samples are compared to assess the reproducibility of the anisotropy measurements.

2.2. Crystal Growth

Single crystalline samples of PSBS with a series of m values are grown by a combination of modified Bridgman and self-flux methods. The growth process is complicated, because these compounds do not exhibit congruent melting [9]. To grow high-quality single crystals, the following steps are taken: High-purity raw material shots of Pb (99.998%), Bi (99.9999%), and Se (99.999%) are sealed in a quartz tube that was heat-treated beforehand. For removing oxidization layers formed in air on the raw shots of Pb and Bi, surface cleaning procedures are performed; Pb shots are annealed in hydrogen atmosphere, and Bi shots are washed with diluted HNO_3. Based on the phase diagram reported by Shelimova

et al. [9], we choose the starting composition of PbSe:Bi_2Se_3 = 45:55 in molar ratio. The raw materials are reacted and homogenized in a melt held at 1173 K for 6 h, and the crystal growth was fostered by slowly sweeping the temperature from 1023 K to 923 K at a rate of 2 K/hour in a temperature gradient of roughly 1 K/cm. At the beginning of the growth, $m = 1$ crystals are formed at the low-temperature end of the melt, which causes the composition of the melt to become PbSe-poor. As the temperature is lowered and the crystals growth proceeds, the melt becomes more and more PbSe-poor and the composition of the grown crystals changes from $m = 1$ to higher m values.

3. Results : Grown Crystals

After cutting the grown boule [Fig. 1a] with a wire saw, cleavable single crystals can be separated. The phase of each piece is determined by the 2θ–θ XRD analysis on a cleaved surface. Even when the appearance of the surface is clean and shiny, the XRD profile can sometimes contain peaks from multiple phases; we discard such multi-phase crystals and only use those crystals that show single-phase peaks on both top and bottom surfaces for further characterizations. The largest size of the single-phase crystal we obtained was roughly $2 \times 1 \times 0.2$ mm^3. The XRD pattern confirmed that the cleavage plane is along the *ab*-plane. Note that, because the crystal structures of the PSBS homologous series are monoclinic [13], the *c*-axis is *not* perpendicular to the *ab*-plane, and hence the direction normal to the *ab* plane is called c^*-axis. This means that the 2θ–θ XRD profile on a cleaved surface of a PSBS single crystal reflects the periodicity along the c^*-axis, which corresponds to $c \sin\beta$ with c and β the *c*-axis lattice constant and the angle between the *c*-axis and the *ab*-plane, respectively. The periodicities (i.e. the $c \sin\beta$ values) for m = 1, 2, and 3 are obtained in the present experiments to be 1.5795(19), 2.5287(11), and 3.4753(15) nm, respectively [Fig. 1b-d and Table 1] [14]; these results are consistent with those previously reported [9, 13]. However, in addition to these three phases, we found a new phase of unknown XRD profile, as shown in Fig. 1e. The crystals of this new phase presents a shiny cleavage plane, and the appearance is indistinguishable from other PSBS phases nor the Bi_2Se_3 compound. Nevertheless, from the XRD profile, the periodicity perpendicular to the cleavage plane is calculated to be 4.4274(15) nm, which is very long and is obviously different from any known phase in this Pb-Bi-Se ternary system. The detailed XRD data for all four phases are presented in the Supplementary Materials.

In the PSBS compound, an increase in m corresponds to an increase in the thickness of the Bi_2Se_3 layer. In fact, when m increases by one from $m = 1$ to 2 and from m = 2 to 3, the $c \sin\beta$ value increases by 0.9492 and 0.9466 nm, respectively; these values are close to 0.9545 nm, the thickness of the QL unit of bulk Bi_2Se_3. In this respect, the difference in $c \sin\beta$ between the $m = 3$ phase and the new phase is 0.9521 nm, which is also close to the QL-unit thickness of Bi_2Se_3, suggesting that the new phase corresponds to the $m = 4$ phase of the homologous series. This systematics is graphically confirmed by plotting $c \sin\beta$ vs. m (assuming that the new phase is $m = 4$), which clearly presents

Composition $(PbSe)_5(Bi_2Se_3)_{3m}$	$d_{\mathrm{PbSe-PbSe}}$ ($= c \sin\beta$; nm)	$\Delta d_{\mathrm{PbSe-PbSe}}$ (nm)
$m = 1$	1.5795(19)	–
$m = 2$	2.5287(11)	0.9492
$m = 3$	3.4753(15)	0.9466
New phase ($m = 4$)	4.4274(15)	0.9521

Table 1: $\Delta d_{\mathrm{PbSe-PbSe}}$ is the increment in $d_{\mathrm{PbSe-PbSe}}$ ($= c \sin\beta$) when m increases by one.

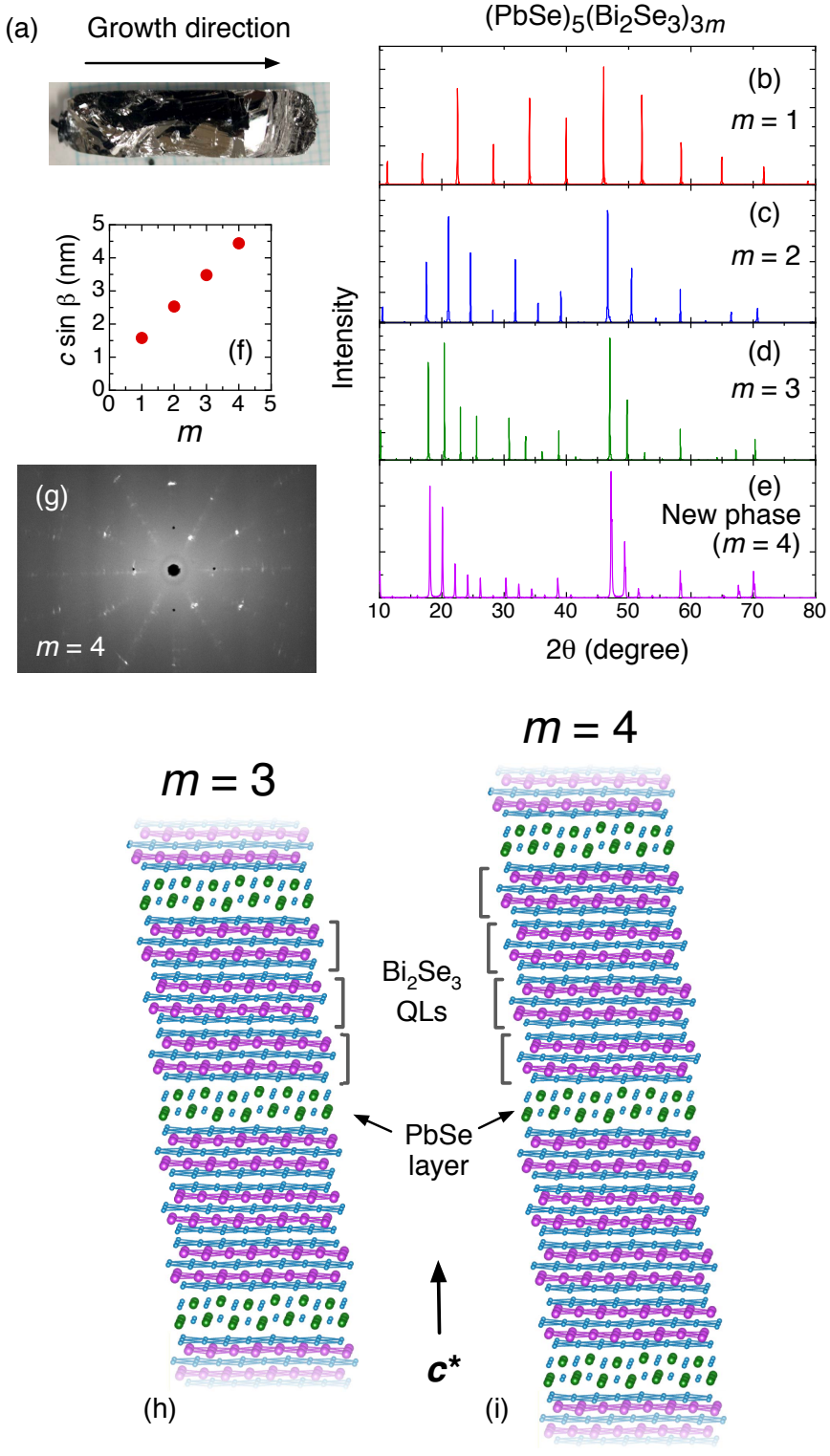

Figure 1: (a) Photograph of the boule grown from the raw composition of PbSe:Bi_2Se_3 = 45:55. (b-e) 2θ–θ XRD profiles taken on cleaved surfaces of single-crystal samples of the PSBS homologous series with various m values: (b) $m = 1$; (c) $m = 2$; (d) $m = 3$; (e) new phase, $m = 4$. (f) Plot of $c \sin \beta$ vs. m, where the data point from the new phase is assigned to $m = 4$. (g) A Laue picture taken on the cleaved surface of a single crystal of the $m = 4$ phase. (h, i) Schematic pictures of the crystal structures drawn [20] for the $m = 3$ and 4 phases of the PSBS homologous series. Because of the monoclinic structure, the direction normal to the cleavage plane (ab-plane) is denoted as c^*-axis.

a linear relation [Fig. 1f]. Figure 1g shows a Laue picture taken on the *ab*-plane of a single crystal of the $m = 4$ phase. The same pattern is obtained from any spot on the surface, which confirms the single-crystal nature of the sample. The Laue picture clearly shows three-fold symmetry and is very similar to that of the $m = 2$ and 3 phases. We show schematic pictures of the crystal structures for $m = 3$ and 4 in Fig. 1h and 1i; these pictures are drawn by expanding the crystal structure data for $m = 2$ [13].

We have further analyzed the crystal structure of the new phase with single-crystal X-ray apparatus with CCD imaging. The space group is identified to be monoclinic P2 with the Laue class $2/m$. The lattice parameters are $a = 2.167(3)$ nm, $b = 0.4123(5)$ nm, $c = 4.431(8)$ nm, $\beta = 93.35(5)^\circ$, and $c \sin\beta = 4.424(9)$ nm. The values of a and b are close to those reported for $m = 1$ and 2 [13], and $c \sin\beta$ is in good agreement with that obtained from the 2θ–θ analysis. It is useful to note that β is closer to 90° than that for smaller m [9], and this is naturally explained by the elongated c unit while keeping a and b units to be essentially unchanged. Further refinement was tried both for powder and single-crystal XRD data, but it was difficult because the crystals are relatively soft and easily deformed, and also because the PSBS system appears to be metastable and the $m = 4$ homologous phase disappears upon grinding. More detailed information on this X-ray analysis is presented in the Supplementary Materials.

To quantitatively determine the actual compositions of the grown crystals, inductively coupled plasma atomic emission spectroscopy (ICP-AES) analysis is employed. The results for all the grown phases, including the new phase, are shown in Table 2, in which the Se contents are fixed to the stoichiometric values calculated from the formula $(PbSe)_5(Bi_2Se_3)_{3m}$; namely, the Se contents are set to be 14, 23, 32, and 41 for $m = 1$, 2, 3, and 4, respectively, and the Pb and Bi contents are calculated against these values, because the ICP-AES analysis is best at giving relative ratios between constituent elements. One can see that the Pb content is much smaller than the nominal value of 5 in all the compounds. In contrast, the Bi content is always larger than the nominal values. These results point to the existence of high densities of Bi antisite defects, $Bi^{\bullet}_{Pb}$, and in fact, the summed values of Pb and Bi contents (shown as "Pb+Bi" in Table 2) are in reasonable agreement with the nominal values. Therefore, the cation/anion ratios obtained by the ICP-AES analyses support the conclusion that all four phases are members of the PSBS homologous series.

The above ICP-AES results indicate that the actual chemical formula for PSBS had better be expressed as $(Pb_xBi_ySe)_5(Bi_2Se_3)_{3m}$ (note that the solubility of Pb into Bi_2Se_3 is reported to be negligible [15]). We show in Table 3 the x and y values in this formula for $m = 1$ – 4 calculated from the ICP-AES results. The $Bi^{\bullet}_{Pb}$ antisites are donors to provide n-type carriers, and thus one can calculate the expected n-type carrier density from the charge imbalance $\Delta q = 5(2x + 3y - 2)$ per mol; this formula is based on the valence states Pb^{2+}, Bi^{3+}, and Se^{2-}. Positive Δq corresponds to n-type. The expected carrier density n_e is obtained by dividing Δq by the unit-cell volume, and for $m = 4$, one obtains $n_e = 2 \times 10^{20} - 4 \times 10^{20}\,\mathrm{cm}^{-3}$.

m	Nominal composition	Pb	Bi	Pb+Bi	Se
1	$Pb_5Bi_6Se_{14}$	3.38(10)	7.47(3)	10.9(7)	14
2	$Pb_5Bi_{12}Se_{23}$	3.25(6)	13.6(2)	16.8(1)	23
3	$Pb_5Bi_{18}Se_{32}$	2.77(11)	20.2(4)	23.0(3)	32
4	$Pb_5Bi_{24}Se_{41}$	3.26(7)	25.5(2)	28.8(1)	41

Table 2: The data are obtained from ICP-AES analyses. The selenium composition is fixed to be $5+9m$.

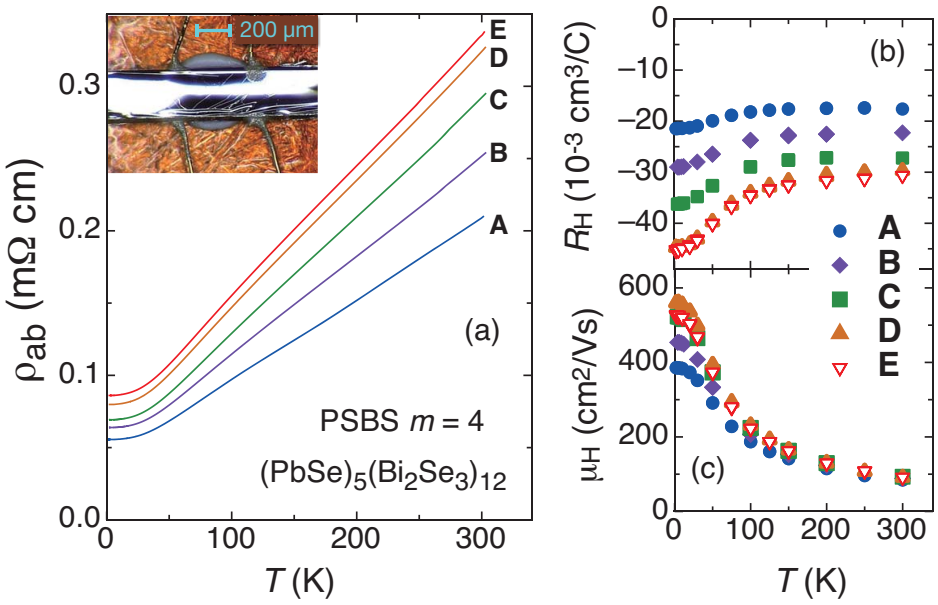

Figure 2: Transport properties of the new compound, $Pb_5Bi_{24}Se_{41}$ (PSBS $m = 4$), measured on five different pieces of single crystals (A–E). Panels (a)-(c) present the temperature dependences of (a) ρ_{ab}, (b) R_H, and (c) μ_H. The inset of panel (a) shows a photograph of sample C with four voltage contacts.

4. Results : Transport Properties

Figure 2a shows the temperature dependences of ρ_{ab} for five samples of PSBS $m = 4$ single crystals obtained from the same boule. The temperature dependence is metallic, and the absolute value of ρ_{ab} varies by about 40% between samples. The temperature dependences of R_H for the same set of samples are shown in Fig. 2b; the variation of R_H between samples is again about 40% at room temperature. It is useful to note that the data in Fig. 2b tell us that the sample-to-sample variation in ρ_{ab} is caused essentially by a change in the carrier density, which is presumably related to different levels of Bi antisite defects in different pieces of crystals. In fact, as shown in Fig. 2c, the Hall mobility μ_H calculated from ρ_{ab} and R_H for those samples converges at room temperature, indicating that the level of electron scattering is unchanged among samples at room temperature. The carrier density n_H calculated from R_H varies from 1×10^{20} cm^{-3} to 3×10^{20} cm^{-3}, which is smaller than that expected from the density of Bi antisites by roughly a factor of two. A major part of this discrepancy is probably due to the Hall factor, which accounts for the difference between the actual carrier density and that calculated from $1/(eR_H)$, because the latter can vary due to the multiband effects and the relaxation-time anisotropy.

The out-of-plane resistivity ρ_{c^*} is useful for evaluating the anisotropy and the dimensionality of the charge transport. In Fig. 3a, the temperature dependences of ρ_{c^*} for the

m	x (Pb)	y (Bi)	Δq (per mol)
1	0.68(2)	0.29(1)	1.0–1.3
2	0.65(1)	0.31(3)	0.8–1.6
3	0.55(2)	0.45(8)	1.1–3.3
4	0.65(1)	0.30(3)	0.7–1.4

Table 3: The x and y values quantify the off-stoichiometry in terms of the formula $(Pb_xBi_ySe)_5(Bi_2Se_3)_{3m}$ determined from the ICP-AES analysis for each m. Δq gives the charge imbalance per mole due to the off-stoichiometry calculated by $\Delta q = 5(2x+3y-2)$; in this table, because of the errors in x and y values, the ranges of Δq dictated by the errors are shown.

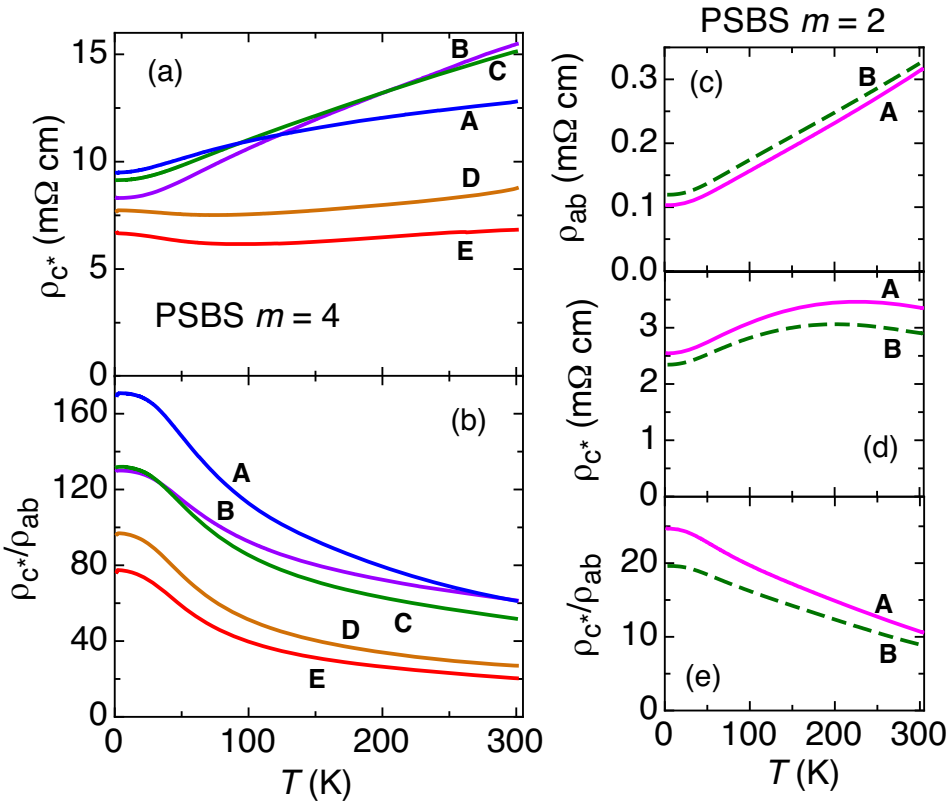

Figure 3: (a-b) Temperature dependences of (a) ρ_{c^*} and (b) ρ_{c^*}/ρ_{ab} measured on the same $m = 4$ samples (A–E) as those shown in Fig. 2. (c-e) Temperature dependences of (c) ρ_{ab}, (d) ρ_{c^*}, and (e) ρ_{c^*}/ρ_{ab} measured on two $m = 2$ samples (A and B).

same set of samples as those in Fig. 2 are shown. The magnitude of ρ_{c^*} is of the order of 10 mΩcm, which is large for a degenerate semiconductor with $n_e \simeq 1 \times 10^{20}$ cm^{-3}. The temperature dependence is either weakly metallic or almost temperature independent, from which it is difficult to judge whether the transport along the c^*-axis is coherent. Nevertheless, as shown in Fig. 3b, the anisotropy ratio ρ_{c^*}/ρ_{ab} grows with lowering temperature and reaches 75–170 at low temperature, which points to the quasi-two-dimensional nature of the transport [16]. For comparison, we show in Fig. 3c-e the data of ρ_{ab}, ρ_{c^*}, and ρ_{c^*}/ρ_{ab} for two samples of PSBS $m = 2$ single crystals. One can see that ρ_{ab} is comparable to that of the $m = 4$ phase, but ρ_{c^*} (and hence ρ_{c^*}/ρ_{ab}) is much smaller in the $m = 2$ phase. Thus, the present results suggest that the transport anisotropy increases with increasing m in the PSBS homologous series. (We note that it has so far been difficult to obtain sufficiently large single crystals of the $m = 3$ phase, and hence we do not have reliable data for the resistivity anisotropy for $m = 3$.)

5. Discussions

To understand the implications of the difference in the resistivity anisotropy between $m = 2$ and 4, it is useful to remember that in bulk Bi_2Se_3, which can be viewed as the $m \to \infty$ limit of the PSBS homologous series, the anisotropy is as small as ∼3 [17], and this is because Bi_2Se_3 has a 3D ellipsoidal Fermi surface. Therefore, the *increase* in the anisotropy for larger m cannot be an indication that the system is approaching the $m \to \infty$ limit. In other words, the present result on the resistivity anisotropy strongly supports the conjecture that PbSe layer in this homologous series works as a block layer for the charge transport. Nevertheless, the volume density of the PbSe layer becomes

smaller for larger m, and hence the larger ρ_{c^*} value at $m = 4$ cannot be due simply to the presence of PbSe layers as series resistors.

One possibility to understand the trend in the resistivity anisotropy is to consider that the level of hybridization between the top and bottom interface states of topological origin within each Bi_2Se_3 layer plays an important role in determining the out-of-plane transport. In such a case, a thicker Bi_2Se_3 layer (i.e. a larger m) means weaker hybridization, which would lead to smaller transfer integral between top and bottom interface states within the Bi_2Se_3 layer, resulting in a larger c^*-axis resistivity. Although speculative, this possibility suggests the importance of the topological interface state in the out-of-plane transport in the PSBS homologous series.

We now discuss the chemical reason why it was possible to synthesize the $m = 4$ phase in the present work. According to the phase diagram of the PbSe-Bi_2Se_3 pseudo-binary system reported by Shelimova *et al.* [9], there are only three stable phases, $Pb_5Bi_6Se_{14}$ ($m = 1$), $Pb_5Bi_{12}Se_{23}$ ($m = 2$), and $Pb_5Bi_{18}Se_{32}$ ($m = 3$), which respectively form below 993, 973, and 948 K. The phase diagram also suggests that if the Bi_2Se_3:PbSe ratio is higher than that corresponds to $m = 3$, a mixed phase solidifies below 930 K. However, this phase diagram was constructed from only a finite number of compositional data points, and it is possible that there is a narrow compositional window in which the $m = 4$ phase preferentially grows below some temperature that lies between 930 and 948 K. In our growth method for this homologous series, the composition of the melt changes continuously toward a higher Bi_2Se_3:PbSe ratio as the temperature is lowered and the crystal growth proceeds, which must have brought the system to hit the right composition/temperature window for the $m = 4$ growth. Hence, our method is suitable for the growth of rare compounds in a homologous series, although it is difficult to obtain large single crystals for each phase.

Finally, it would be useful to elaborate on the difference in the crystal structures of the homologous series obtained for Pb-Bi-Se and Pb-Bi-Te ternary systems. The Pb-Bi-Te ternary system also gives rise to a homologous series, but its construction is fundamentally different from that obtained for the Pb-Bi-Se ternary system. Namely, in the case of tellurides, although the composition formula is superficially similar to the selenides and is written as $(PbTe)_m(Bi_2Te_3)_n$ (m and n are integers), in this homologous series "PbTe" is incorporated into the original rhombohedral structure of Bi_2Te_3, forming a covalently-bonded Te-Bi-Te-Pb-Te-Bi-Te septuple-layer unit [18, 19]. Hence, in the telluride homologous series, the rhombohedral symmetry of the crystal structure which stems from a cubic structure distorted along (111) direction is essentially unchanged from that of Bi_2Te_3. Importantly, the $(m, n) = (1, 1)$ phase of this telluride homologous series, $PbBi_2Te_4$, which simply consists of a stack of the Te-Bi-Te-Pb-Te-Bi-Te septuple-layers, is known to be a topological insulator [18, 19]; hence, the telluride homologous series is a heterostructure of two topological insulators (i.e. $PbBi_2Te_4$ and Bi_2Te_3) and the topological states show up only on the surrounding surface. In contrast, in the selenide homologous series [7, 8, 9, 13], PbSe is not incorporated into the rhombohedral structure of Bi_2Se_3 and the rock-salt structure of bulk PbSe partly remains, forming the PbSe layer of square symmetry; this layer alternates with the Bi_2Se_3 layer of hexagonal symmetry, and the resulting structure is no longer rhombohedral. As is already emphasized, this selenide homologous series is a heterostructure of a topological insulator and an ordinary insulator, and hence its electronic nature is fundamentally different from that of the telluride homologous series.

6. Conclusions

We have synthesized a new compound in the $(PbSe)_5(Bi_2Se_3)_{3m}$ homologous series with $m = 4$, which became possible by using a melt-growth method in which the composition of the melt changes continuously to allow the whole series of compounds to grow in a sequential manner. This new compound, $Pb_5Bi_{24}Se_{41}$, is a member of the unique family of topological materials in which alternating layers of the topological insulator Bi_2Se_3 and the ordinary insulator PbSe form natural heterostructures, leading to the appearance of topological interface states throughout the bulk. The trend in the c^*-axis resistivity and the resistivity anisotropy with increasing m values suggests that the hybridization of the topological interface states plays an important role in the out-of-plane transport in this compound.

Acknowledgment

We acknowledge the Comprehensive Analysis Center, ISIR, Osaka University, for technical supports in the CCD X-ray diffraction analysis. We also thank T. Toba for technical assistances. This work was supported by JSPS (KAKENHI 25220708, 24540320, and 25400328), MEXT (Innovative Area "Topological Quantum Phenomena" KAKENHI 22103004), and AFOSR (AOARD 124038).

References

References

[1] M.Z. Hasan, C.L. Kane, Rev. Mod. Phys. 82 (2010) 3045.

[2] X.-L. Qi, S.-C. Zhang, Rev. Mod. Phys. 83 (2011) 1057.

[3] Y. Ando, J. Phys. Soc. Jpn. 82 (2013) 102001.

[4] Moore, J. Nature 464 (2010) 194.

[5] H. Peng, W. Dang, J. Cao, Y. Chen, D. Wu, W. Zheng, H. Li, Z. X. Shen, Z. Liu, Nat. Chem. 4 (2012) 281.

[6] R.J. Cava, H. Ji, M.K. Fuccillo, Q.D. Gibson, Y.S. Hor, J. Mater. Chem. C 1 (2013) 3176.

[7] Kanatzidis, M.G. Acc. Chem. Res. 38 (2005) 359.

[8] Y. Zhang, A.P. Wilkinson, P.L. Lee, S.D. Shastri, D. Shu, D.-Y. Chung, M.G. Kanatzidis, J. Appl. Cryst. 38 (2005) 433.

[9] L.E. Shelimova, O.G. Karpinskii, V.S. Zemskov, Inorg. Mater. 44 (2008) 927.

[10] Y. Xia, D. Qian, D. Hsieh, L. Wray, A. Pal, H. Lin, A. Bansil, D. Grauer, Y.S. Hor, R.J. Cava, M.Z. Hasan, Nat. Phys. 5 (2009) 398.

[11] K. Nakayama, K. Eto, Y. Tanaka, T. Sato, S. Souma, T. Takahashi, K. Segawa, Y. Ando, Phys. Rev. Lett. 109 (2012) 236804.

[12] Y. Zhang, K. He, C.-Z. Chang, C.-L. Song, L.-L. Wang, X. Chen, J.-F. Jia, Z. Fang, X. Dai, W.-Y. Shan, S.-Q. Shen, Q. Niu, X.-L. Qi, S.-C. Zhang, X.-C. Ma, Q.-K. Xue, Nat. Phys. 6 (2010) 584.

[13] L. Fang, C.C. Stoumpos, Y. Jia, A. Glatz, D.Y. Chung, H. Claus, U. Welp, W.K. Kwok, M.G. Kanatzidis, arXiv:1307.0260 (2013).

[14] Strictly speaking, the actual c value must be doubled for $m = 2$, because the unit cell is twice as large in this phase along c [13].

[15] I.I. Aliev, K.N. Babanly, N.B. Babanly, Inorganic Materials 44 (2008) 1179.

[16] Y. Nakamura, S. Uchida, Phys. Rev. B 47 (1993) 8369.

[17] M. Stordeur, K.K. Ketavong, A. Priemuth, H. Sobotta, V. Riede, Phys. Stat. Sol. 169 (1992) 505.

[18] S. Souma, K. Eto, M. Nomura, K. Nakayama, T. Sato, T. Takahashi, K. Segawa, Y. Ando, Phys. Rev. Lett. 108 (2012) 116801.

[19] S.V. Eremeev, G. Landolt, T.V. Menshchikova, B. Slomski, Y.M. Koroteev, Z.S. Aliev, M.B. Babanly, J. Henk, A. Ernst, L. Patthey, A. Eich, A.A. Khajetoorians, J. Hagemeister, O. Pietzsch, J. Wiebe, R. Wiesendanger, P.M. Echenique, S.S. Tsirkin, I.R. Amiraslanov, J. Hugo Dil, E.V. Chulkov, Nat. Commun. 3 (2012) 635.

[20] K. Momma, F. Izumi, J. Appl. Crystallogr. 44 (2011) 1272.